COBEM 2021 26th International Congress of Mechanical Engineering
November 22-26, 2021, Virtual Congress, Brazil

COB-2021-0145
CONSTRUCTAL DESIGN APPLIED TO A MICROCHANNEL WITH TWO MOUNTED TRAPEZOIDAL BLOCKS SUBJECTED TO LAMINAR BOILING FLOWS

Bruno Costa Feijó[a]
Grégory Rodrigues Muniz[b]
Liércio André Isoldi[c]
School of Engineering, Universidade Federal do Rio Grande - FURG, Av Itália, Km 8, s/n, CEP 96203-900, Rio Grande, RS, Brazil.
[a] bruno.feijo1989@gmail.com
[b] gregorymuniz@hotmail.com
[c] liercioisoldi@furg.br

Luiz Alberto Oliveira Rocha
Mechanical Engineering Graduate Program, Universidade do Vale do Rio dos Sinos, Av. UNISINOS, 950, CEP 93.022-750, São Leopoldo, RS, Brazil.
luizor@unisinos.br

Sylvie Lorente
Department of Mechanical Engineering, Villanova University, PA 19085, USA.
sylvie.lorente@villanova.edu

Elizaldo Domingues dos Santos
Universidade Federal do Rio Grande (FURG), Av Itália, Km 8, s/n, CEP 96203-900, Rio Grande, RS, Brazil.
elizaldosantos@furg.br

Abstract. *Microchannel heat exchangers are used in several areas such as refrigeration and air conditioning, electronics and microelectronics, power generation industry, process industry, bioengineering, among others. The present work aims to study the geometric configuration of a microchannel with two trapezoidal blocks mounted in an alternate form on its surfaces subjected to laminar boiling flows. Constructal Design method and Exhaustive Search are used for geometrical investigation of the blocks. Here, a computational fluid dynamics (CFD) code based on the Finite Volume Method (FVM) is used to simulate of the boiling flow. The multi-phase Mixture model and the Lee model for phase change are employed. A microchannel with a length of 1.5 mm and a height of 0.1 mm is simulated. The walls of this microchannel have a temperature of 573 K, and fluid, water in its liquid phase, enters the microchannel with a temperature of 372 K at atmospheric pressure. Two different mass fluxes of 1.0 and 100.0 kg/(m².s) are considered at the inlet of the domain. Along the microchannel, part of the water is heated and boiled. Here, it is investigated the influence of the height and higher width of the first block (H_{11}/L_{11}) over the heat transfer rate and pressure drop for different magnitudes of the ratio between the lower width and higher width (L_{12}/L_{11}). The second block is maintained fixed. Results indicated that the design of the first block has a greater influence over the pressure drop in the microchannel than over the heat transfer rate for the present fluid dynamic and thermal conditions.*

Keywords: *heat transfer, boiling flow, microchannel, numerical study, Constructal Design*

1. INTRODUCTION

An important problem in engineering is the need to dissipate the excessive heat generated by many systems (machines, equipment, plants, among others) due to their operation. Exploring ways to mitigate the problem of heat dissipation, the study of flows in heatsink channels and microchannels has been the subject of several works. Microchannels consist of various small channels that together form a single structure through which a fluid flows confined and dissipates the heat generated (Ohadi *et al.*, 2012). They are present in heat exchangers in refrigeration systems, in electronics and microelectronics, in process industries, in power generation systems, among several other applications (Ohadi *et al.*, 2012; Siddiqui and Zubair, 2017; Rai *et al.*, 2018).

Within the field of study of heatsink channels and microchannels, the study of the phase change of the flowing fluid stands out, especially that of forced convective boiling flows. The boiling of the fluid is associated with the formation of bubbles on the surface regions of the channels when the fluid reaches a temperature above its boiling point. This process can result in an increase in the heat transfer coefficient and thus cause an increase in the heat transfer rates (Collier and

Thome, 1994; Rohsenow *et al*., 1998; Incropera *et al*., 2007). This characteristic can make the boiling of flows inside channels and microchannels attractive for systems that require high rates of heat dissipation. Despite the possible advantages of using boiling, its numerical modeling and geometric evaluation processes still present many challenges and potential for improvements, mainly due to the high complexity of the physical phenomena involved (Kandlikar *et al*., 1999; Khan and Fartaj, 2010; Karayiannis and Mahmoud, 2017).

In the field of design of flow systems, the Constructal Design method has been widely used to show how the design of any animate or inanimate systems can be predicted deterministically by a physical principle of maximization of access of internal currents (Bejan and Lorente, 2008; Bejan and Zane, 2012; Bejan and Lorente, 2013; Bejan, 2020). The Constructal Theory is a mental view that the evolution of the design in flow systems follows the Constructal Law of design and evolution, which states that "the design evolves in such a way as to facilitate access to the currents that flow into this system" so that these systems continue to exist throughout of time. A boiling flow within a heatsink channel is a clear example of this type of system. Constructal Design has been successfully employed as a powerful tool to study the design in engineering problems, as channel flows (Bello-Ochende *et al*., 2009; Song *et al*., 2015; Feijó *et al*., 2018; Moreira *et al*., 2021). With the application of the method, it is possible to evaluate the influence of the channel geometry over the flow and heat transfer by defining the search space of geometrical configurations, and in this way, propose improvements to the channel design. However, it is important to state that the Constructal Design is not a geometric optimization methodology. For this purpose of geometric optimization, Exhaustive Search was employed, consisting of the simulation of all geometric possibilities from the defined search space, considering some step of variation between the simulated geometries.

The present study will employ a computational fluid dynamics (CFD) software, ANSYS Fluent™ 18.1, based on the finite volume method (FVM) to solve convective boiling flow problems inside microchannels. Mixture multiphase model and Lee's phase change model were used. The microchannel studied has two trapezoidal blocks, one on the upper surface and the other on the lower one, to increase the interaction between the flow and the microchannel walls to enhance heat transfer. The microchannel walls are heated and cause the fluid to boil along the microchannel length. Constructal Design was applied to the microchannel geometry as four degrees of freedom and two constraints were set. Exhaustive Search was applied for the geometrical optimization. A multi-objective approach was carried for the geometric evaluation of the microchannel, considering both the thermal and the fluid dynamics objectives simultaneously.

2. MATHEMATICAL MODELING

The problem studied is a two-dimensional microchannel containing two trapezoidal blocks (Figure 1) through which a fluid flows, water initially in its liquid state, which is heated and due to boiling, is partially transformed into vapor. The water enters the microchannel at 372 K of temperature in two different situations studied in this work: with a mass flux of 1.0 and 100.0 kg/(m².s), corresponding to the Reynolds numbers of 0.1 and 10.0, respectively. The volume fractions of the liquid and vapor phases at the channel's inlet are equal to 1 and 0 respectively. The outlet of the microchannel is at atmospheric pressure (P_{out} = 0 atm) while the walls are heated with a constant temperature of T_w = 573 K, including the two blocks. The fluid is considered incompressible and the surfaces of the channel and blocks are non-slip and impermeable (u = v = 0 m/s). The saturation temperature considered is equal to T_{sat} = 373.15 K, the surface tension of water is s = 0.072 N/m and the microchannel has an operating pressure of P = 1 atm.

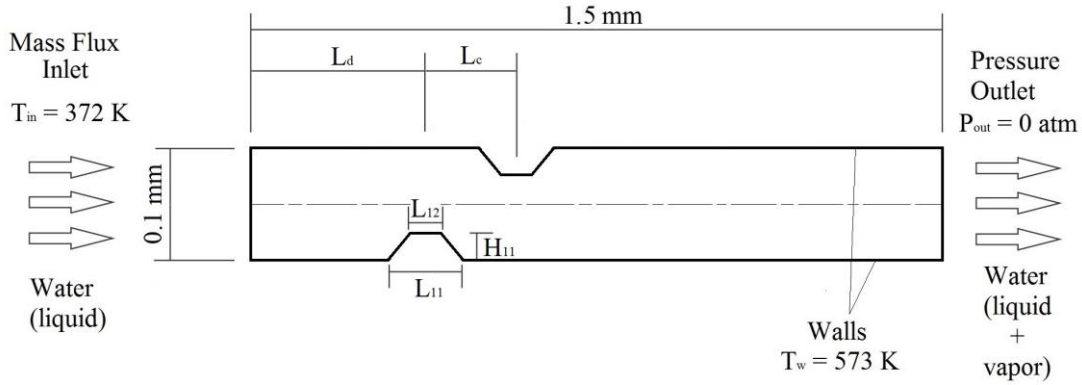

Figure 1 – Computational domain of the microchannel with two heated trapezoidal blocks.

Regarding the dimensions of the microchannel, it has a length of L = 1.5 mm, height of H = 0.1 mm, L_d = 0.4 mm and L_c = 0.2 mm. The Constructal Design method was applied to the geometrical evaluation of the microchannel. The problem is subjected to four degrees of freedom: ratio between the height and higher width of both blocks and ratio between the lower and higher widths of the trapezoidal blocks. In the present study, it is investigated the influence of the height and higher width of the first block (H_{11}/L_{11}) over the heat transfer rate (q) and the pressure drop (ΔP) for different magnitudes

of the ratio between the lower width and higher width (L_{12}/L_{11}). The main purposes are the maximization of the heat transfer rate between the microchannel and the fluid and the minimization of the pressure drop in the microchannel. The heat transfer rate can be calculated as (Chen, 1966):

$$q = A_s h_l (T_w - T_{in}) + A_s h_{NB} (T_w - T_{sat}) \quad (1)$$

where A_s is the microchannel's surface area (m²), h_l is the heat transfer coefficient for the liquid phase flowing alone in the microchannel (W/m².K) and h_{NB} is the nucleate boiling heat transfer coefficient (W/m².K).

The pressure drop in the microchannel can be computed as:

$$\Delta P = P_{in} - P_{out} \quad (2)$$

where P_{in} and P_{out} are the averaged pressures in the inlet and outlet surfaces of the microchannel (Pa), respectively.

The problem is subjected to two constraints (areas of blocks 1 and 2), which both were set to a constant value of 2,000 μm². The area of block 1 can be defined as:

$$A_{B1} = \frac{(L_{11}+L_{12})}{2} . H_{11} \quad (3)$$

where H_{11} is the height of the first block, L_{11} is the higher width of the first block and L_{12} is the lower width of the first block.

Exhaustive Search was applied so that the degrees of freedom are varied in the range: $0.1 \leq H_{11}/L_{11} \leq 2.0$ and $0.1 \leq L_{12}/L_{11} \leq 1.0$. The dimensions of the second block are constant in this study and are defined by $H_{21}/L_{21} = 0.50$ and $L_{22}/L_{21} = 0.50$.

To perform the geometric evaluation process, L_{12}/L_{11} was first varied, keeping H_{11}/L_{11} fixed. The maximum value found for the heat transfer rate was called the once maximized rate, $q_{1,max}$, and the corresponding L_{12}/L_{11} was called the once thermally optimized $(L_{12}/L_{11})_{o,T}$. A minimum value was also found for the pressure drop between the inlet and outlet of the channel, $(\Delta P)_{1,min}$, corresponding to $(L_{12}/L_{11})_{o,F}$. In a second step, the process is repeated for different values of H_{11}/L_{11}. Now, among all simulations, the maximum heat transfer rate is the twice maximized, $q_{2,max}$, and the smallest pressure drop is twice minimized, $(\Delta P)_{2,min}$. Regarding the optimal geometries, this step also obtains the ratio H_{11}/L_{11} once optimized for the thermal objective and another once optimized ratio for the fluid dynamics objective, $(H_{11}/L_{11})_{o,T}$ and $(H_{11}/L_{11})_{o,F}$. In the same way, it is obtained the twice optimized ratios $(L_{12}/L_{11})_{oo,T}$ and $(L_{12}/L_{11})_{oo,F}$. Subsequently, the geometric evaluation will be made taking into account the multi-objective (thermal and fluid dynamics, simultaneously) with the intent of obtaining the optimum multi-objective geometry: $(L_{12}/L_{11})_{oo}$ and $(H_{11}/L_{11})_{o}$. This process is performed for the two mass fluxes studied.

The present study employed the Mixture multiphase model. Unlike the Volume of Fluid model (VOF), Mixture considers the phases as interpenetrating. It is a suitable model for the simulation of multiphase flows in channels where thermofluidic performance is more important than a detailed tracking of the interface between the phases. This model calculates the conservation equations for the mixture of the phases, the equation of the volume fraction for the secondary phases and also has algebraic expressions for the relative and drift velocities. The continuity conservation equation is obtained considering the mixture of the phases and is given by:

$$\frac{\partial}{\partial t}(\rho_m) + \nabla \cdot (\rho_m \vec{V}_m) = 0 \quad (4)$$

where ρ_m is the mixture density (kg/m³) and $\vec{V}_m$ is the mass-averaged velocity (m/s), which are given, respectively, by:

$$\rho_m = \sum_{k=1}^{n} \alpha_k \rho_k \quad (5)$$

$$\vec{V}_m = \frac{\sum_{k=1}^{n} \alpha_k \rho_k \vec{V}_k}{\rho_m} \quad (6)$$

where n is the number of phases, α_k, ρ_k and $\vec{V}_k$ are the volume fraction, density and velocity of phase k.

The momentum conservation equation is also obtained considering the mixture:

$$\frac{\partial}{\partial t}(\rho_m \vec{V}_m) + \nabla \cdot (\rho_m \vec{V}_m \vec{V}_m) = -\nabla p + \nabla \cdot (\mu_m \nabla \vec{V}_m) + \rho_m \vec{g} + \vec{F} - \nabla \cdot \left(\sum_{k=1}^{n} \alpha_k \rho_k \vec{V}_{dr,k} \vec{V}_{dr,k}\right) \quad (7)$$

where p is the pressure (Pa), $\vec{F}$ is a body force (N/m³), $\vec{g}$ is the gravity aceleration (m/s²) and μ_m is the dynamic viscosity of the mixture (N.s/m²). $\vec{V}_{dr,k}$ is the drift velocity for secondary phase k (m/s) and can be expressed as follows:

$$\vec{V}_{dr,k} = \vec{V}_k - \vec{V}_m \tag{8}$$

The energy conservation equation for the mixture can be written as:

$$\frac{\partial}{\partial t}\sum_{k=1}^{n}(\alpha_k \rho_k E_k) + \nabla \cdot \sum_{k=1}^{n}\left[\alpha_k \vec{V}_k (\rho_k E_k + p)\right] = \nabla \cdot \left(k_{eff} \nabla T\right) + S_E \tag{9}$$

where k_{eff} is the effective conductivity ($\sum \alpha_k k_k$), being k_k is the thermal conductivity of phase k (W/m.K), S_E includes any other volumetric heat sources. For a compressible phase, the energy term E_k (J) is given by:

$$E_k = h_k - \frac{p}{\rho_k} + \frac{V_k^2}{2} \tag{10}$$

and $E_k = h_k$ and for an incompressible phase, where h_k is the sensible enthalpy for phase k (J).

The volume fraction equation is expressed based on the continuity conservation equation for the secondary phase. For a primary phase named q and a secondary named p, it can be written as:

$$\frac{\partial}{\partial t}\left(\alpha_p \rho_p\right) + \nabla \cdot \left(\alpha_p \rho_p \vec{V}_m\right) = -\nabla \cdot \left(\alpha_p \rho_p \vec{V}_{dr,p}\right) + \sum_{q=1}^{n}\left(\dot{m}_{qp} - \dot{m}_{pq}\right) \tag{11}$$

where $\dot{m}_{qp}$, $\dot{m}_{pq}$ are the rates of mass transfer between the phases (kg/m³.s).

A very important concept of the Mixture model is the relative (or slip) velocity. It is defined as the relative velocity between two phases:

$$\vec{V}_{pq} = \vec{V}_p - \vec{V}_q \tag{12}$$

Because the phases velocities are unknown at principle, the relative velocity needs to be expressed in an algebraic expression, given by Manninen *et al*. (1996):

$$\vec{V}_{pq} = \frac{\tau_p}{f_{drag}} \frac{(\rho_p - \rho_m)}{\rho_p} \vec{a} \tag{13}$$

where τ_p is the particle relaxation time (s), d_p is the diameter of the particles (or droplets or bubbles) of secondary phase (m), $\vec{a}$ is the secondary phase particle's acceleration (m/s²). The default drag function f_{drag} is defined by the correlation of Schiller and Naumann (1935):

$$f_{drag} = \begin{cases} 1 + 0.15Re^{0.687} & Re \leq 1000 \\ 0.0183Re & Re > 1000 \end{cases} \tag{14}$$

The Reynolds number in Eq. (14) is calculated based on the relative velocity, $\vec{V}_{pq}$ (Manninen *et al*., 1996):

$$Re = \frac{d_p \rho_q |\vec{V}_{pq}|}{\mu_q} \tag{15}$$

Now, from Equations (6), (8) and (12), it is possible to formulate a relation between the relative and the drift velocities:

$$\vec{V}_{dr,p} = \vec{V}_{pq} - \sum_{k=1}^{n} c_k \vec{V}_{kq} \tag{16}$$

where c_k is the mass fraction for any phase (k) and is defined as:

$$c_k = \frac{\alpha_k \rho_k}{\rho_m} \tag{17}$$

In the case of a problem with only two phases, Eq. (16) can be written in a simpler manner:

$$\vec{V}_{dr,p} = \vec{V}_{pq}\left(1 - c_p\right) \tag{18}$$

To simulate the boiling process, Lee's model was employed (Lee, 1980). This model is governed by an equation that takes into account the heat transfer from both the liquid to the vapor (evaporation) and vapor to liquid (condensation) phases:

$$\frac{\partial}{\partial t}(\alpha_v \rho_v) + \nabla \cdot \left(\alpha_v \rho_v \vec{V}_v\right) = \dot{m}_{lv} - \dot{m}_{vl} \tag{19}$$

where v and l represent the vapor and liquid phases respectively, $\dot{m}_{lv}$ and $\dot{m}_{vl}$ are the rates of mass transfer due to evaporation and condensation (kg/m³.s), respectively. They are given by (Lee, 1980):

$$\begin{cases} \dot{m}_{lv} = coef\ f * \alpha_l \rho_l \frac{(T_l - T_{sat})}{T_{sat}} & If\ T_l \geq T_{sat}\ (evaporation) \\ \dot{m}_{lv} = 0 & If\ T_l < T_{sat} \end{cases} \tag{20}$$

$$\begin{cases} \dot{m}_{vl} = coef\ f * \alpha_v \rho_v \frac{(T_{sat} - T_v)}{T_{sat}} & If\ T_v \leq T_{sat}(condensation) \\ \dot{m}_{lv} = 0 & If\ T_v > T_{sat} \end{cases} \tag{21}$$

where *coef f* is the time relaxation parameter for the Lee's model (s^{-1}). It's value has a wide range and it must be fine tuned with previously known data in each case in order to achieve reliable results.

3. NUMERICAL MODELING

The present study used the ANSYS Fluent™ 18.1 software to perform the numerical simulations. The software uses the finite volume method (FVM) to solve the equations. For the pressure-velocity coupling, the SIMPLE scheme was used. For spatial discretization, a Green-Gauss Cell Based gradient and the QUICK method were used for the moment, energy and volume fraction equations. For pressure, Body Force Weighted spatial discretization was used. The simulations were carried out in a steady state regime and the residuals were considered converged when reaching the value of 1.0×10^{-5} for continuity, 1.0×10^{-6} for velocities and volume fraction and 1.0×10^{-7} for energy.

A mesh independence study was carried out based on the case with the geometry considered the most complex in terms of the simulation (H_{11}/L_{11} = 2.0 and L_{12}/L_{11} = 1.0 with Re_H = 10.0), as shown in Table 1. Considering the mesh as independent when the relative deviation of the heat transfer rate between two successive meshes was less than 0.03% ($R = \left|(q^j - q^{j+1}/q^j)\right| < 3 \times 10^{-4}$), it was observed that the mesh with 38,382 finite volumes met this criterion. All meshes have triangular volumes and have an extra refinement in the vicinity of the walls along the entire microchannel, as shown in Figure 2.

Table 1. Mesh independence study.

Number of Volumes	q (W)	Relative Deviation
7,595	6,165.700	0.01629
12,275	6,065.214	0.00427
16,150	6,039.288	0.00997
21,046	5,979.053	0.00366
27,630	6,000.921	0.00144
38,382	6,009.571	0.00024
49,811	6,011.021	-

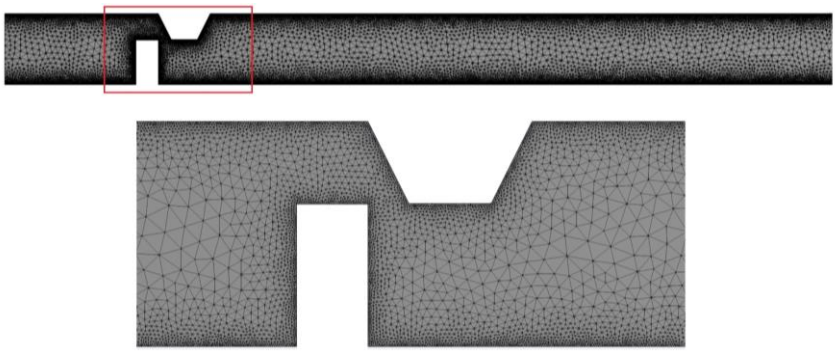

Figure 2 - Mesh with triangular finite volumes employed in the present study.

In order to verify the model used, a comparison was made with the results obtained in the work of Vivekanand and Raju (2015), where the boiling flow of water inside a microchannel was simulated in the laminar regime, in microchannels with the height of 0.1 mm and length of 1.0 mm, in two different situations: with fixed temperature in the walls and with

constant heat flux in the walls. The comparison of the vapor volume fraction generated along the microchannel can be seen in Figure 3 for the case with prescribed temperature in the walls and constant heat flux, Figs. 3(a) and 3(b), respectively. In general, the differences observed were less than 4%, and therefore, the model was considered adequate to reproduce boiling flows in the laminar regime inside microchannels.

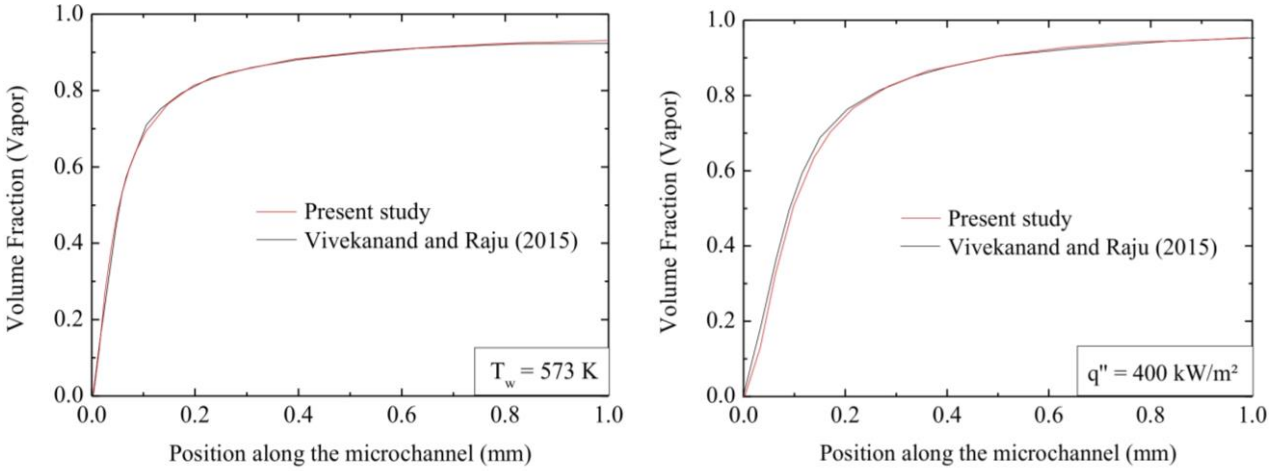

Figure 3 - Verification of the model employed in this study with that of Vivekanand and Raju (2015): a) case study with prescribed temperature at the channel walls, b) case study with prescribed heat flux.

4. RESULTS

4.1 Thermal Analysis

First, the geometric evaluation is performed considering only the thermal objective, the maximization of heat transfer rate (q). Figure 4 shows the results obtained from the effect of L_{12}/L_{11} over the heat transfer rate for different values of H_{11}/L_{11}, in cases with Re_H = 0.1 and 10. It is possible to observe different behaviors from L_{12}/L_{11} and H_{11}/L_{11} by comparing the two values of Re_H studied. For Re_H = 0.1, there was a noticeable difference in the heat transfer rate between the two values of H_{11}/L_{11} when L_{12}/L_{11} = 0.1. With the increase of L_{12}/L_{11}, from 0.25 onwards, this difference tended to decrease until practically nonexistent difference for L_{12}/L_{11} = 1.0. For Re_H = 10, however, there was a much greater distinction of the heat transfer rate observed between H_{11}/L_{11} = 0.1 and 2.0. It is also noticeable that for H_{11}/L_{11} = 0.1 the heat transfer rate was hardly affected by the variation of L_{12}/L_{11}. The highest differences between the best and worst cases are nearly 2.0 % and 10.0 % for Re_H = 0.1 and 10.0, respectively.

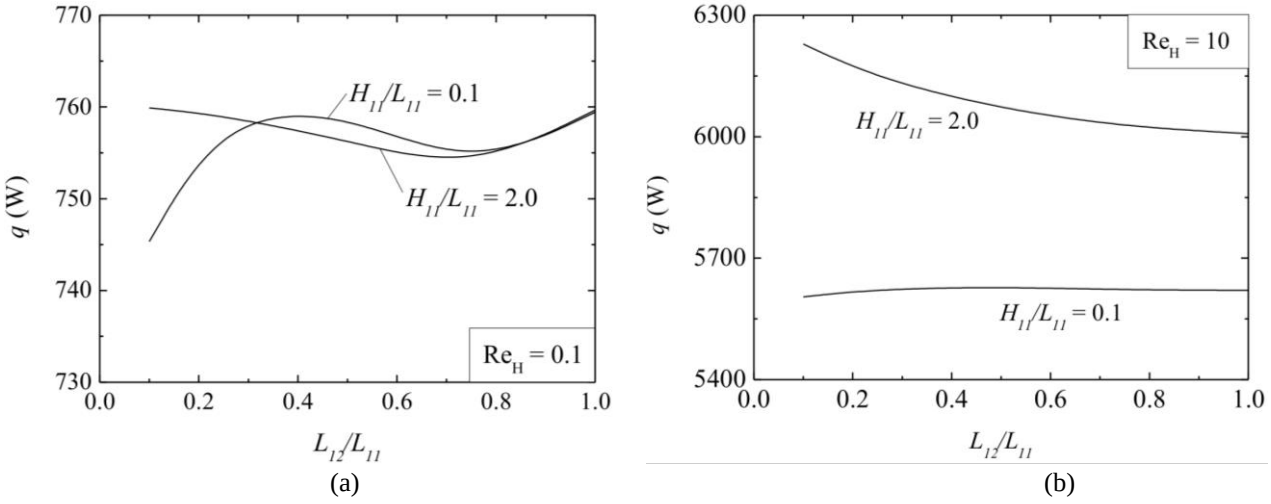

Figure 4 – Effect of L_{12}/L_{11} over the heat transfer rate (q) for different values of H_{11}/L_{11} and Reynolds number Re_H = 0.1 (a) and 10 (b).

From these results, it was possible to obtain the values of the optimal thermal geometries, $(H_{11}/L_{11})_{o,T}$ = 2.0 and $(L_{12}/L_{11})_{oo,T}$ = 0.1, the same for both values of Re_H, with a $q_{2,max}$ = 759.88 W and $q_{2,max}$ = 6,229.01 W for Re_H = 0.1 and 10 respectively.

Figure 5 shows the temperature and the vapor volume fraction fields for two different cases, H_{11}/L_{11} = 0.1 and 2.0 with L_{12}/L_{11} = 0.1 and Re_H = 10. It is possible to observe that there is a higher concentration of vapor close to the channel walls as this is the region with the highest temperatures. In H_{11}/L_{11} = 2.0, it is apparent that the higher height of the block causes a slight accumulation of vapor at its base compared to H_{11}/L_{11} = 0.1. The higher height of the block forced a greater interaction between the flow and the heated walls, explaining the difference in the heat transfer rate observed in Figure 4 (b) between H_{11}/L_{11} = 0.1 and 2.0. The volume fraction fields also illustrate that the variation of the ratio H_{11}/L_{11} affected the length of channel required for change of phase from water to vapor.

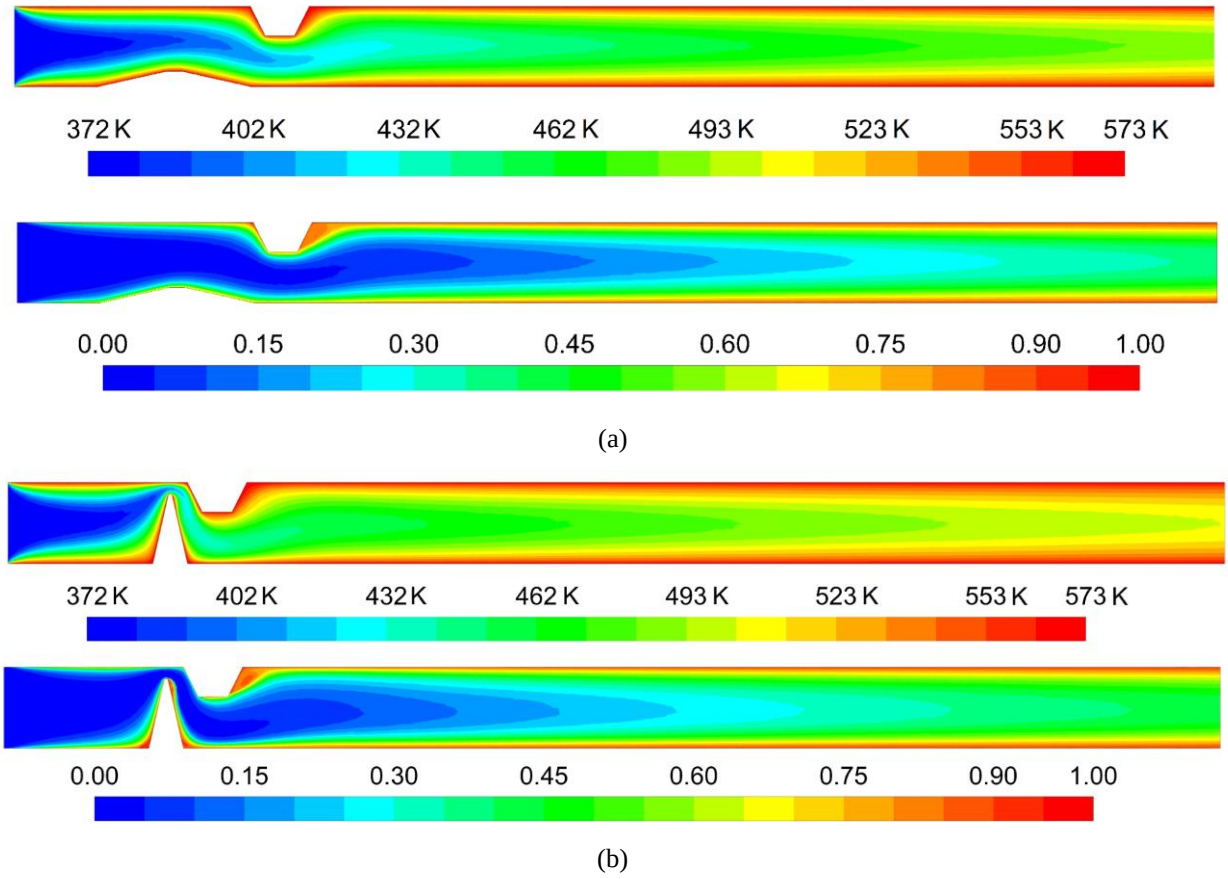

Figure 5 – Temperature (K) and Vapor Volume Fraction fields for Re_H = 10, L_{12}/L_{11} = 0.1 and: a) H_{11}/L_{11} = 0.1, b) H_{11}/L_{11} = 2.0.

4.2 Fluid Dynamics Analysis

In this step, the analysis is repeated considering now the fluid dynamic objective, the minimization of the pressure drop (ΔP) along the microchannel. As can be seen in Figure 6, L_{12}/L_{11} and H_{11}/L_{11} behaviors were similar in relation to the two values of Re_H. In both cases, the change in L_{12}/L_{11} had practically no effect on the pressure drop for H_{11}/L_{11} = 0.1, with the minimum values observed with L_{12}/L_{11} = 0.1. For H_{11}/L_{11} = 2.0, the pressure drop was significantly greater compared to H_{11}/L_{11} = 0.1, obtaining minimum values of pressure drop with intermediate values of L_{12}/L_{11} in both situations. The optimum fluid dynamic geometries were $(H_{11}/L_{11})_{o,F}$ = 0.1 and $(L_{12}/L_{11})_{oo,F}$ = 0.1, the same for the two cases of mass flux. In regards to the minimum values of the pressure drop found, these were $(\Delta P)_{2,min}$ = 2.01 Pa for Re_H = 0.1 and $(\Delta P)_{2,min}$ = 200.69 Pa for Re_H = 10.

The velocity and pressure fields for two cases with Re_H = 0.1 are shown in Figure 7. In contrast to what was seen in the thermal analysis, the fluid dynamic analysis allows us to observe that there are significant differences in the velocities and pressures present in the microchannel with increasing the block's height. The greater height of H_{11}/L_{11} = 2.0 causes a stricture of the fluid, significantly increasing its velocity when passing through the blocks and consequently increasing the pressure drop along the microchannel, therefore proving to be a much worse geometry from the fluid dynamic perspective.

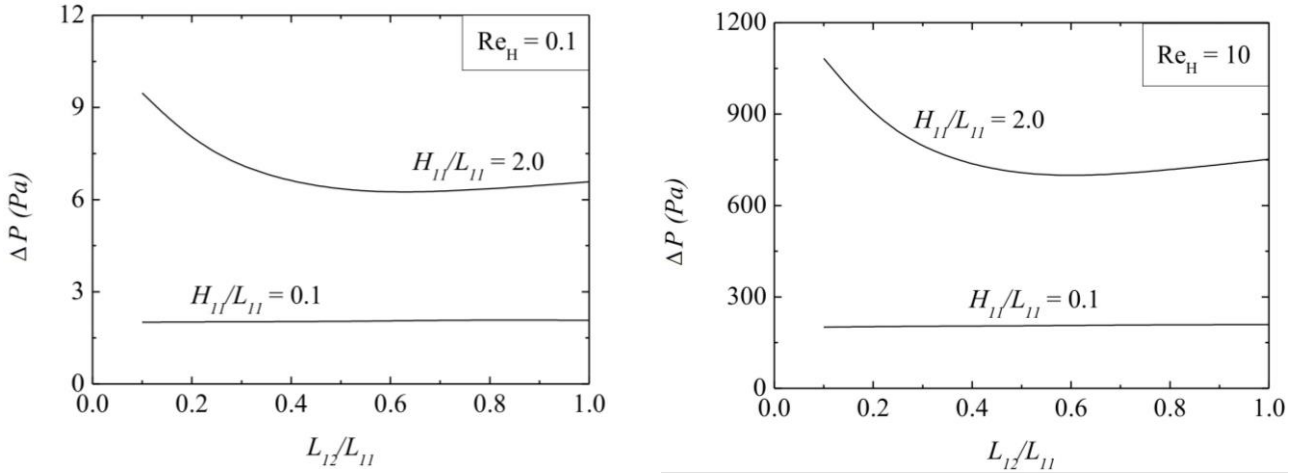

Figure 6 – Effect of L_{12}/L_{11} over the pressure drop (ΔP) for different values of H_{11}/L_{11} and Reynolds number Re_H = 0.1 (a) and 10 (b).

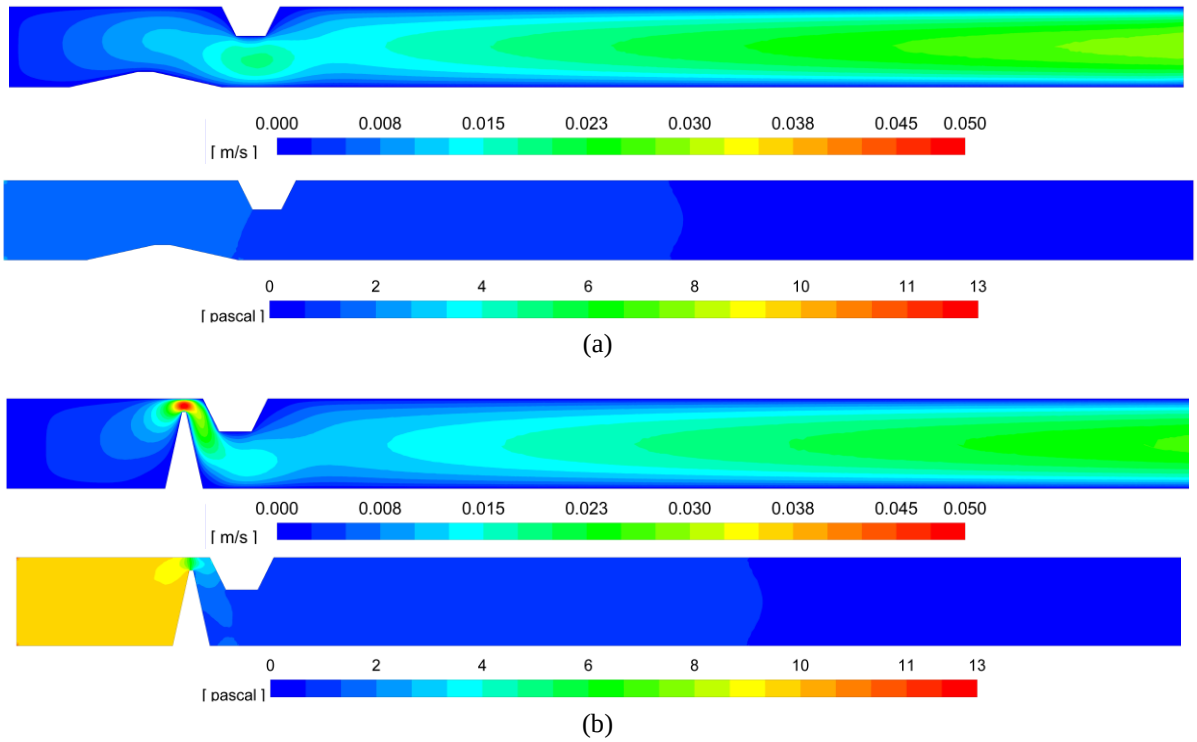

Figure 7 – Velocity (m/s) and Pressure (Pa) fields for Re_H = 0.1, L_{12}/L_{11} = 0.1 and: a) H_{11}/L_{11} = 0.1, b) H_{11}/L_{11} = 2.0.

4.3 Multi-objective Analysis

This last part of the geometric evaluation is carried out considering simultaneously the two objectives, thermal and fluid dynamic, in order to determine the optimum multi-objective geometry. Here, it is plotted the pressure drop (ΔP) as a function of the inverse of the heat transfer rate (q). The best multi-objective results are those closest to the point where both axis are equal to zero, that is, the minimum pressure drop and the maximum heat transfer rate as possible. It can be seen from Figure 8 that H_{11}/L_{11} = 0.1 is clearly superior from a multi-objective point of view compared to H_{11}/L_{11} = 2.0, for both Reynolds numbers studied. It is possible to verify that among the geometries analyzed in this study, their variation causes a much greater effect in the pressure drop than in the heat transfer rate, which is notable in the fact that the optimal multi-objective geometries found are the same optimum fluid dynamic geometries.

As Figure 8 shows, for Re_H = 0.1 there is practically no difference in heat transfer rate between H_{11}/L_{11} = 0.1 and 2.0, as seen in the thermal analysis, in comparison with the variation of pressure drop. With the increase of the Reynolds number, to Re_H = 10, it is possible to spot the appearance of a difference in the heat transfer rate between the two optimal

multi-objective geometries of H_{11}/L_{11} = 0.1 and 2.0, however this difference is still small when compared to the effect of the geometry in the pressure drop.

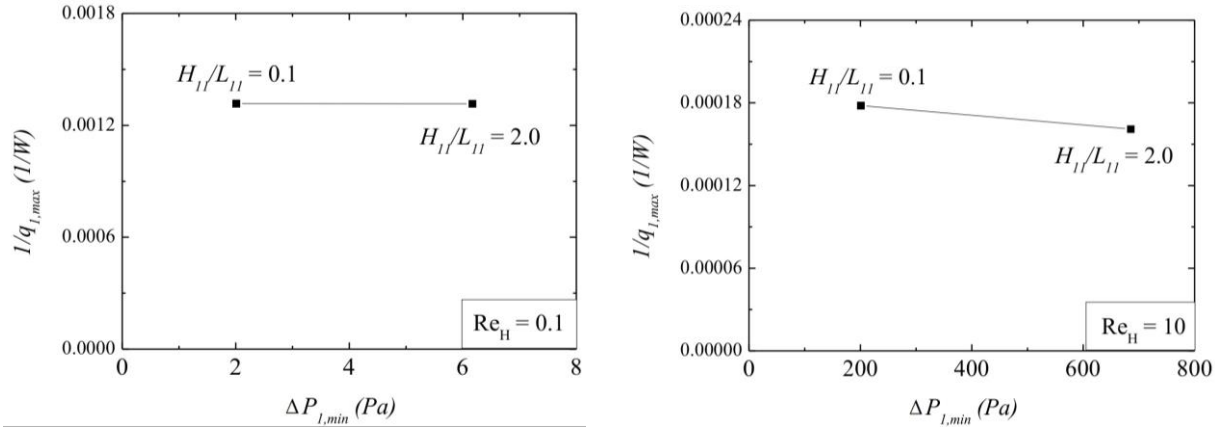

Figure 6 – Effect of the once minimized pressure drop $(\Delta P)_{1,min}$ over the inverse of the once maximized heat transfer $(1/(q)_{1,max})$for different values of H_{11}/L_{11} and Reynolds number Re_H = 0.1 (a) and 10 (b).

Table 2 shows the overall optimal multi-objective geometries from the results obtained in this study:

Table 2. Optimal shapes for multi-objective problem

Re_H	0.1	10
$(H_{11}/L_{11})_o$	0.1	0.1
$(L_{12}/L_{11})_{oo}$	0.1	0.1
H_{11}	19.07 µm	19.07 µm
L_{11}	190.69 µm	190.69 µm
L_{12}	19.07 µm	19.07 µm

5. CONCLUSIONS

The present numerical study applied the Constructal Design method and Exhaustive Search to the geometric evaluation of a microchannel with two trapezoidal blocks and its walls heated to 573 K, in which a boiling flow passed through. The working fluid used was water and its flow was in the laminar regime and two mass fluxes values were studied: 1.0 and 100.0 kg/(m².s), corresponding to Re_H = 0.1 and 10, respectively. It was investigated the influence of the height and higher width of the first block (H_{11}/L_{11}) over the heat transfer rate (q) and the pressure drop (ΔP) for different magnitudes of the ratio between the lower width and higher width of the trapezoidal block (L_{12}/L_{11}). The configuration of the second block was constant in all cases. The objectives of the geometric evaluation were to find geometries that would maximize the heat transfer rate (q) and minimize the pressure drop (ΔP). Thermal and fluid dynamics analyzes were carried out, as well as a multi-objective analysis. In total, 20 simulations were performed with the software ANSYS Fluent™ 18.1.

The results obtained allowed us to conclude that, for the conditions applied in this study, the influence of L_{12}/L_{11} over the pressure drop was only significant for the cases with the highest height of the block, H_{11}/L_{11} = 2.0, where intermediate values have been shown to cause the smallest pressure drops. H_{11}/L_{11} demonstrated to have a great influence on the pressure drop, being possible to observe through the velocity and pressure fields that the greater height of the first block caused a stricture effect, significantly increasing the pressure drop of the flow when crossing the blocks region. Regarding the thermal analysis, it was possible to verify that H_{11}/L_{11} caused an increase in the heat transfer rate for Re_H = 10, where its highest value, H_{11}/L_{11} = 2.0, provided the highest heat transfer rates due to the greater interaction between the fluid and the blocks. Fluid dynamics proved dominant in the geometric evaluation of this study, with the degrees of freedom analyzed, H_{11}/L_{11} and L_{12}/L_{11}, having a much greater influence over the pressure drop than over the heat transfer rate. Because of this, the optimal multi-objective geometries found were exactly the same optimum geometries found when considering only the fluid dynamic objective, $(H_{11}/L_{11})_o$ = 0.1 and $(L_{12}/L_{11})_{oo}$ = 0.1 for both Reynolds numbers. It was observed that with the increase of the Reynolds number to Re_H = 10, there was a slight increase in the share of heat transfer in the multi-objective, which leads to the conclusion that there is a possibility that an increase in the Reynolds number above this value can lead to an augmentation of this trend. Another important aspect noticed is concerned with the length

of channel required to change of phase from water to vapor, which was significantly affected by the first block configuration, mainly the ratio H_{11}/L_{11} in the present investigation.

This study proved that the design of the blocks can be highly important for thermal and fluid dynamic performance of microchannels, as well as over the phase of change, which was not previously investigated using the Constructal Design method. For future studies, other ratios and fluid flow conditions will be investigated.

6. ACKNOWLEDGEMENTS

The authors L.A. Isoldi, L.A.O. Rocha and E.D. dos Santos thank CNPq – Conselho Nacional de Desenvolvimento Científico e Tecnológico for research grant (Processes: 306012/2017-0, 307791/2019-0, 306024/2017-9). G.R. Muniz thanks FAPERGS – Fundação de Apoio à Pesquisa do Estado do Rio Grande do Sul for scientific initiation scholarship and PET - Programa de Educação Tutorial from the Mechanical Engineering program in FURG. E.D. dos Santos also thanks FAPERGS for financial support by the Public Call Nº 05/2019 – PqG (Grant number: 19/2551-0001847-9).

7. REFERENCES

Bejan, A., 2020. *Freedom and Evolution*. Cham, Switzerland, Springer.

Bejan, A., Lorente, S., 2013. "Constructal law of design and evolution: Physics, biology, technology, and society". *Journal of Applied Physics*. Vol. 113, No. 151301.

Bejan, A., Lorente, S., 2008. *Design with Constructal Theory*, Hoboken Wiley.

Bejan, A., Zane, J. P., 2012. *Design in Nature*. New York, USA: Doubleday.

Bello-Ochende, T., Meyer, J. P., Bejan, A., 2009. "Constructal Ducts with wrinkled entrances". *International Journal of Heat and Mass Transfer*, Vol. 52, pp. 3628-3633.

Chen, J. C., 1966. "Correlation for Boiling Heat Transfer to Saturated Fluids in Convective Flow". *Industrial and Engineering Chemistry Process Design and Development*, Vol. 5, pp. 322.

Collier, J.G., Thome, J.R., 1994. *Convective Boiling and Condensation*. 3rd ed., Clarendon Press, Oxford, United Kingdom.

Incropera, F.P., Dewitt, D.P., Bergman, T.L., Lavin, E.A.S., 2007. *Fundamentos de Transferência de Calor*. 6th Ed. (in portuguese), John Wiley and Sons, Hoboken, New Jersey, USA.

Feijó, B.C., Lorenzini, G., Isoldi, L.A., Rocha, L.A.O., Goulart, J.N.V., Dos Santos, E.D., 2018. "Constructal design of forced convective flows in channels with two alternated rectangular heated bodies". *International Journal of Heat and Mass Transfer*, Vol. 125, pp. 710-721.

Kandlikar, S.G., Shoji, M., Dhir, V.K., 1999. *Handbook of Phase Change: Boiling and Condensation*. Taylor & Francis, Philadelphia, USA.

Karayiannis, T.G., Mahmoud, M.M., 2017. "Flow boiling in microchannels: Fundamentals and applications". *Applied Thermal Engineering*. Vol. 115, No. 25, pp. 1372-1397.

Khan, M.G., Fartay, A., 2011. "A review on microchannel heat exchangers and potential applications". *Int. J. Energy Res*. Vol. 35, pp. 553–582.

Lee, W.H., 1980. "A Pressure Iteration Scheme for Two-Phase Flow Modeling". *Multiphase Transport Fundamentals, Reactor Safety, Applications*. Washington, DC, USA.

Manninen, M., Taivassalo, V., Kallio, S., 1996. "On the Mixture Model for Multiphase Flow". *VTT Publications*.

Moreira, R.S.M., Escobar, C.C., Isoldi, L.A., Davesac, R.R., Rocha, L.A.O., Dos Santos, E.D., 2021. "Numerical Study and Geometric Investigation of Corrugated Channels Subjected to Forced Convective Flows". *Journal of Applied and Computational Mechanics*. Vol. 7, pp. 727-738.

Ohadi, M., Choo, K., Dessiatoun, S., Cetegen, E., 2012. "Emerging Applications of Microchannels". *Briefs in Applied Sciences and Technology*. pp. 67–105.

Rai, S.K., Sharma, R., Saifi, M., Tyagi, R., Singh, D., Gupta, H., 2018. "Review of recent applications of micro channel in mems devices". *International Journal of Applied Engineering Research*. Vol. 13, No. 9, pp. 64-69.

Rohsenow, W.M., Hartnett, J.P., Cho, Y.I., 1998. *Handbook of Heat Transfer*. 3rd ed. McGraw-Hill. USA.

Schiller, L., Nauman, A., 1935. "A drag coefficient correlation". *VDI Zeitung*, Vol. 77, pp. 318–320.

Siddiqui, O.K., ZuBAIR, S.M., 2017. "Efficient energy utilization through proper design of microchannel heat exchanger manifolds: A comprehensive review". *Renewable and Sustainable Energy Reviews*. Vol. 74, pp. 969–1002.

Song, Y., Asadi, M., Xie, G., Rocha, L.A.O., 2015. "Constructal wavy-fin channels of a compact heat exchanger with heat transfer rate maximization and pressure losses minimization". *Applied Thermal Engineering*, Vol. 75, pp. 24-32.

Vivekanand, S. V. B., Raju, V. R. K., 2015. "Simulation of Evaporation Heat Transfer in Rectangular Microchannel". *Procedia Engineering*, Vol. 127, pp. 309-316.

8. RESPONSIBILITY NOTICE

The authors are the only responsible for the printed material included in this paper.